Approved For Release 2002/07/02 : CIA-RDP78T05439A000500010016-2

SECRET

16857

AN ARMY INTELLIGENCE DOCUMENT

PRELIMINARY ANALYSIS

THE SOVIET MISSILE SYSTEM: GOA (U)

MIS 21-65
MARCH 1965

PREPARED BY
U.S. ARMY MISSILE COMMAND
REDSTONE ARSENAL, ALABAMA

WARNING NOTICE
SENSITIVE SOURCES AND METHODS INVOLVED

[redacted]

EXCLUDED FROM AUTOMATIC REGRADING
DOD DIR 5200.10 DOES NOT APPLY

25X1C

COPY 38 OF 275 COPIES
NUMBER OF PAGES 84

SECRET

*Army and DIA review(s) completed.

SECRET

AN ARMY INTELLIGENCE DOCUMENT

PRELIMINARY ANALYSIS

THE SOVIET MISSILE SYSTEM: GOA (U)

MIS 21-65
MARCH 1965

PREPARED BY

U.S. ARMY MISSILE COMMAND
REDSTONE ARSENAL, ALABAMA

THIS DOCUMENT WAS COMPILED AND PUBLISHED BY THE ARMY MISSILE COMMAND AFTER APPROVAL IN THE OFFICE OF THE ASSISTANT CHIEF OF STAFF FOR INTELLIGENCE AND THEREFORE CONTAINS AGREED DEPARTMENT OF THE ARMY INTELLIGENCE.

WARNING NOTICE
SENSITIVE SOURCES AND METHODS INVOLVED

THIS INFORMATION IS NOT RELEASABLE TO FOREIGN GOVERNMENTS 25X1C

SECRET

(S) FOREWORD (U)

(S) MIS-21-65 presents the results of an engineering analysis of the GOA missile and transporter. Photographs of the missile and transporter as they appeared for the first time in the November 1964 Moscow Parade, and scalings from the photographs, were the basis for the analysis.

(S) This study was prepared by the Directorate of Missile Intelligence, U.S. Army Missile Command, Redstone Arsenal, Alabama with support from the Research and Development Directorate, U.S. Army Missile Command, and the U.S. Army Foreign Science and Technology Center, Washington, D. C.

(U) Comments or queries relating to this report should be addressed to the Commanding General, U. S. Army Missile Command, Redstone Arsenal, Alabama, ATTN: AMSMI-Y.

(S) TABLE OF CONTENTS (U)

(S) LIST OF FIGURES (U)

(S) LIST OF FIGURES (Continued) (U)

(S) LIST OF TABLES (U)

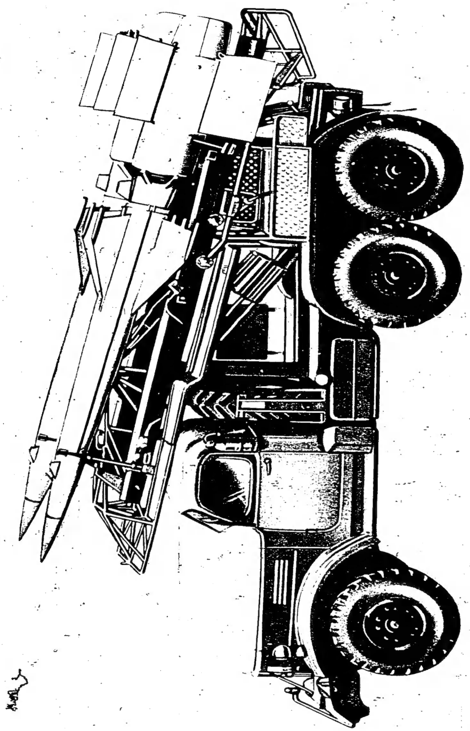

Figure 1. (C) Soviet Missile GOA Mounted on Transporter. (U)

I. (S) INTRODUCTION (U)

(S) The Soviets have developed and deployed a low altitude surface-to-air defensive missile designated by the intelligence community as the GOA. This missile was first displayed in the November 1964 Moscow Parade (Figure 1). The missile is dual mounted on a modified ZIL-157 truck. The transporter/loader vehicle appears equipped with missile checkout equipment and the necessary mechanisms for missile off-loading onto the launchers. This engineering analysis, based upon photographic evidence and photographic interpretation, defines the configuration, performance and operating characteristics of the GOA missile.

(S) The Soviets have deployed the SA-3 missile system (using the GOA missile) to over 100 sites within the Soviet Union (Figures 2, 3, and 4). Although system development was underway in 1959 at the Kapustin Yar Missile Test Range, the missile was not shown until the 7 November 1964 Moscow Parade. The system fire control radar, designated LOW BLOW, has not been seen in detail; nor has a definite ELINT signal been associated with this equipment. A generalized engineering analysis of the two probable guidance schemes can, however, be made on the basis of available information.

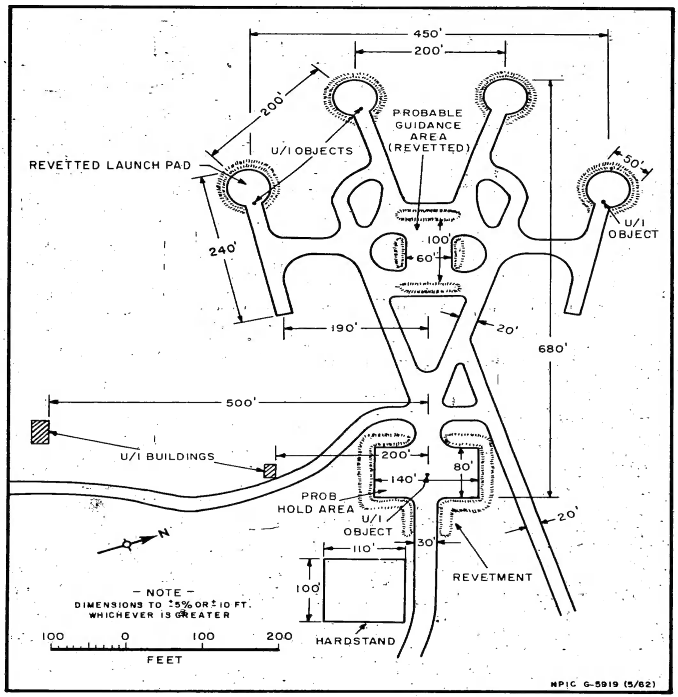

Figure 2. (S) SA-3 Site Configuration. (U)

Figure 3. (S-NOFORN) Photograph of SA-3 Site. (C)

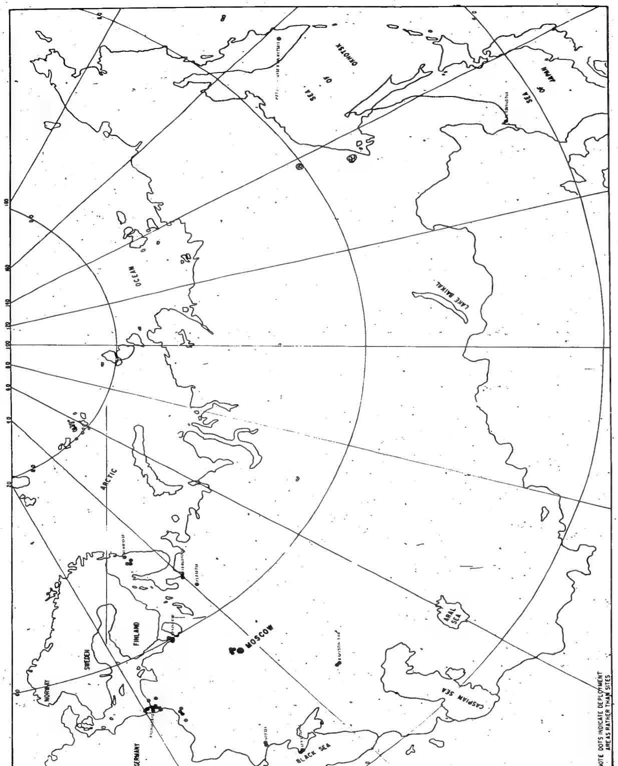

Figure 4. (S) SA-3 System Deployment in USSR. (S)

II. (S) SUMMARY (U)

(S) The GOA surface-to-air missile is a tandem-configured, two-stage vehicle using solid propellant motors in both stages. The missile launch weight is estimated to be about 2050 pounds. The most probable warhead is high explosive with directional fragmentation and weighs about 175 pounds.

(S) Two GOA missiles are mounted on a dual-rail launcher which is probably trainable in both azimuth and elevation.

(S) The missile has a maximum slant-range capability of about 12 nm, and a maximum altitude capability of about 35,000 feet (based on a 2 g maneuver limitation at this altitude). The system minimum altitude capability is unknown, but is not dependent upon missile limitations (beyond missile control dead zone).

SECRET

TABLE 1. (S) SUMMARY OF GOA MISSILE CHARACTERISTICS. (U)

Characteristics	Sustainer and Booster	Sustainer	Booster
Length	19.23 ft	12.42 ft	6.81 ft
Diameter	-	15.2 in	21.2 in
Empty weight	1273 lb	810 lb	463 lb
Propellant weight	777 lb	260 lb	517 lb
Launch weight	2050 lb	1070 lb	980 lb
Warhead weight	-	175 lb HE Frag	-
Propellant type	-	Double base solid	Double base solid
Thrust (sea level)	-	3477 lb	30,500 lb
Specific impulse	-	214 lb-sec/lb	214 lb-sec/lb
Burning time	-	16 sec (average)	3.0-4.3 sec
Maximum velocity	Mach 1.65-1.7	Mach 2.5	-
Maximum effective maneuvering altitude (approximately 2g's)	-	35,000 ft	-
Maximum effective range	-	12 nm (approximate)	-

SECRET

III. (S) CONCLUSIONS (U)

(S) A summary of the GOA missile characteristics is presented in Table 1. The following conclusions are derived from the contents of this report.

A. (S) Propulsion (U)

1. (S) Booster (U)

(S) Booster propulsion is provided by a solid propellant rocket motor probably using an extruded double-base solid propellant similar to that used in the SA-2 booster. This motor would provide an average thrust of approximately 30,500 pounds with a burn-time between 3 and 4.3 seconds depending on nozzle plug adjustment for ambient temperature. The total impulse is sufficient to boost the missile to about Mach 1.65-1.70 at booster burnout. The nozzle plug is manually adjusted prior to launch to partially compensate for variations in the propellant grain temperature and to maintain the thrust level within acceptable limits.

2. (S) Sustainer (U)

(S) The sustainer also has a solid propellant rocket motor which provides an estimated 3500 pounds thrust for an average 16 seconds burntime. The propellant is estimated to be the same as that used in the booster, i.e., an extruded, double-base type. An adjustable plug is also used in the sustainer nozzle to compensate for variation in propellant grain temperatures. Maximum sustainer burn-out velocity has been calculated to be about Mach 2.5.

B. (S) Aerodynamics (U)

(S) Aerodynamic control of the GOA missile is provided by four canard control fins near the nose of the sustainer. Fixed swept-back cruciform fins at the rear of the sustainer, and fold-out, straight wing, cruciform fins on the booster provide stabilization. Aileron surfaces on one pair of sustainer stabilizer fins provide roll control. The tapered forward section of the sustainer body and the boat-tailed booster reduce form and base drag. This detailed attention to drag reduction is necessary to performance in a low altitude mission. All control surfaces are in-line and oriented at an angle of 45 degrees with respect to the pitch and yaw planes. The missile is probably flown in this same relative position to obtain maximum advantage of the control surfaces.

C. (S) Electronics (U)

(S) The identical probable antennas, apparently polyrod type, on each of the sustainer stabilizer fin tips could be used in either a command or a beam rider guidance system. Antennas could be located in the top tunnel over the warhead section or in the open spaces of the rod-like tunnels on the sides of the sustainer. Present information is inconclusive to determine the existence of antennas in either location.

D. (S) Performance (U)

(S) Structural design limitations on maneuver capabilities cannot be determined with a high degree of confidence from presently available information. A maneuver capability limitation of 8 g's appears reasonable and has been used in this study to define the maximum capabilities. The maximum altitude capability of about 35,000 feet has been based on a minimum 2 g maneuver capability at this altitude and the maximum slant range capability of about 12 nm was computed for residual velocities and maneuver capabilities of Mach 1.3 and 2 g, respectively. Minimum altitude intercept capability, unknown at this time, is dependent primarily on the ground based electronics and siting conditions. The missile configuration and characteristics do not limit the system low-altitude capabilities (beyond the missile control dead zone).

E. (S) Warhead (U)

(S) Available space and configuration of the warhead section, and weight and balance estimates, are consistent with a high explosive, directional fragmentation warhead weighing approximately 175 pounds.

F. (S) Transporter (U)

(S) The GOA missile transporter utilizes the ZIL-157 truck as the basic vehicle. Two missiles are secured to individual support beams which are probably utilized to load the missile onto a launcher rail. A fixed tubular rack, separate from the missile support beams, provides ready access to the missile and loading mechanism for missile maintenance, preliminary checkout, and for transloading operations.

IV. (S) DISCUSSION (U)

A. (S) General (U)

1. (S) Dimensions of the GOA missile and transporter are shown in Figures 5 and 6. Some dimensions will probably be refined at a later date. Minor dimensional refinements will not effect the over-all estimated characteristics and performance capabilities of the missile.

2. (S) Photography of the missile does not reveal access hatches or doors, but external conduits, protuberances, and actuator rods are apparent which suggest the locations of various missile components (Figure 7).

B. (S) Propulsion Systems (U)

1. (S) Booster (U)

(S) Boost velocity is achieved using a solid propellant rocket motor.

a. (S) The solid propellant is probably an extruded double-base type identical to the SA-2 booster propellant. Eight propellant sticks of this type can be arranged symmetrically in the motor case (Figure 8). The SA-2 booster propellant characteristics are similar to a U.S. double-base propellant designated for JATO use.

b. (S) The booster motor case appears to be a standard cylinder with semiellipsoidal ends. The likely candidate for the case material is a chrome-vanadium steel such as that designated EI-659 by the Soviets and listed as a material for rocket motors and cases. An allowable design hoop stress for this material would be about 45,000 to 50,000 psi. The case wall thickness, estimated to be about 0.276 inches (7 mm), is compatible with the widths of the machine welds observed in the photography.

c. (S) Insulation is normally required to prevent a loss of case strength due to wall overheating. An insulation thickness of about 0.1 inch limits the temperature rise to about 600°F.

d. (S) The standard converging-diverging booster nozzle is equipped with a plug similar to that of the SA-2. The nozzle plug can be manually adjusted to partially control variations in the

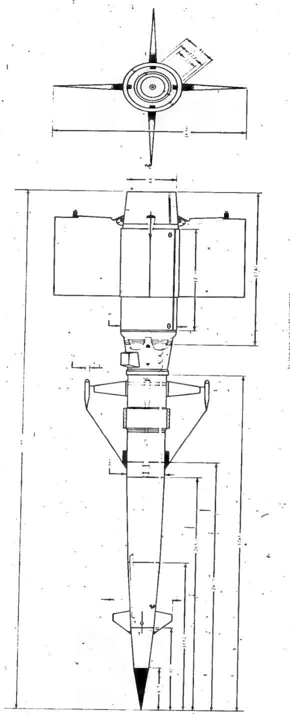

Figure 5. (S) GOA Missile Dimensions. (U)

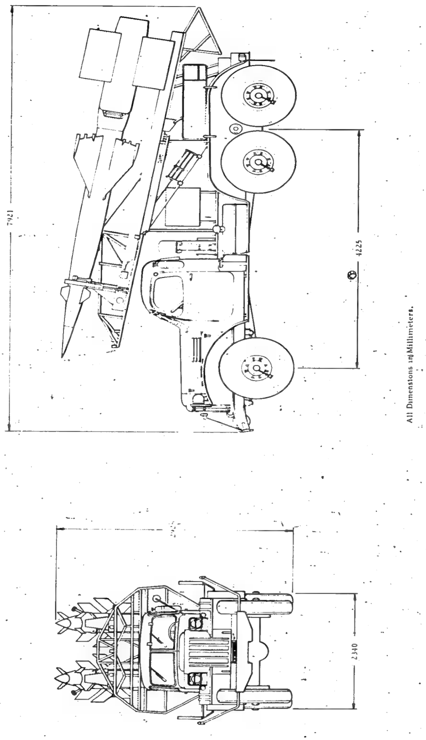

Figure 6. (C) The GOA Transporter Dimensions. (U)

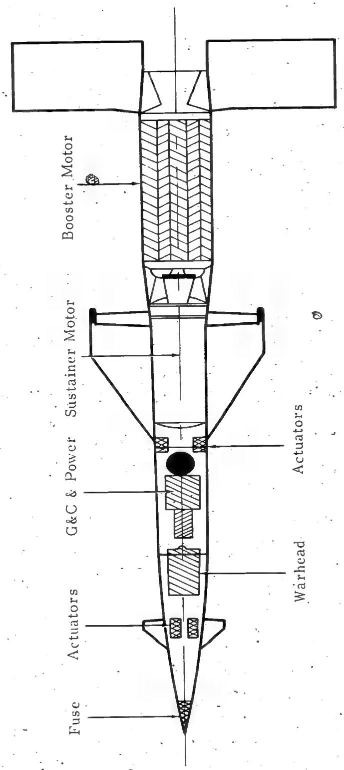

Figure 7. (S) Probable Location of GOA Missile Components. (U)

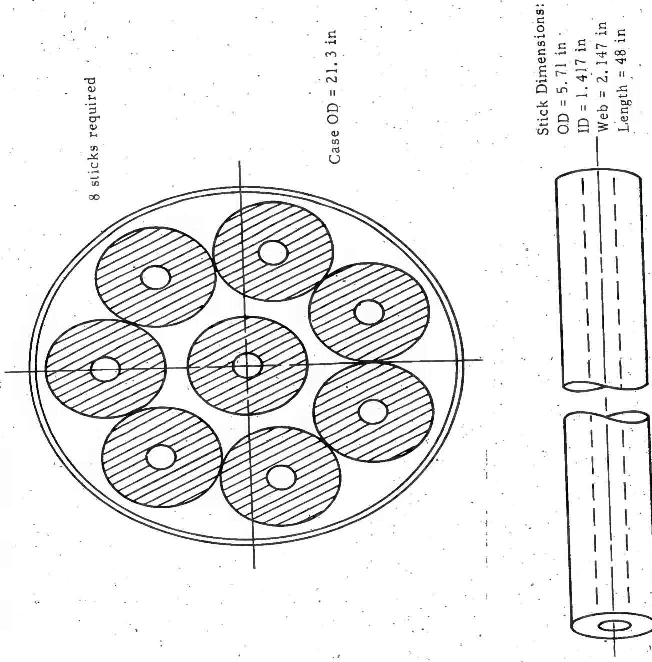

Figure 8. (S) Assumed Booster Grain Design. (U)

TABLE 2

(S) SUMMARY OF ESTIMATED BOOSTER PERFORMANCE (70°F). (U)

Motor weight	834 lb
Propellant weight	517 lb
Propellant	Solid (double-base)
Thrust at sea level	30,480 lb
Burntime	3.6 sec
Specific impulse at sea level	214.5 sec
Total impulse at sea level	111,000 lb-sec

propellant burning rate. The plug permits an adjustment of the throat area to maintain a desired chamber pressure (about 1200 psia), thereby partially compensating for variations in propellant temperatures. A throat insert, probably corundum, may be provided.

e. (S) Estimated booster motor performance data are shown in Table 2. (See Appendix I for computations.)

2. (S) Sustainer (U)

(S) A solid propellant rocket motor provides second stage (sustainer) thrust.

a. (S) The sustainer propellant is believed to be the same double-base type as that used in the booster; with changes in the grain configuration to provide a lower thrust and, consequently, a longer burning time. The estimated internal-burning grain configuration is about 14 inches in diameter and 44 inches long.

b. (S) The sustainer motor case is a cylinder, probably with ellipsoidal ends. The case material is probably the same as that used for the booster motor case. Wall thickness is estimated to be 0.197 inches (5 mm), and wall insulation thickness is estimated to be 0.1 inch.

c. (S) The converging-diverging sustainer nozzle contains a nozzle plug and throat insert similar in design to that of the booster nozzle.

d. (S) Estimated sustainer motor performance was calculated; the results are shown in Table 3. (See Appendix I for computations.)

C. (S) Aerodynamics (U)

(S) Aerodynamic configurations of the GOA missile appear to have been optimized for low altitude intercepts. (See Appendix II for computations.)

1. (S) The missile is a tandem two-stage cruciform configuration with all fins in line and oriented at 45 degrees with respect to the pitch and yaw axes. The three sets of four fins are: canard control fins, clipped-delta stabilized fins, and fold-out, rectangular booster stabilizer fins.

TABLE 3

(S) SUMMARY OF ESTIMATED SUSTAINER PERFORMANCE (70°F). (U)

Motor weight	500 lb
Propellant weight	260 lb
Propellant	Solid (double-base)
Thrust at sea level	3480 lb
Burntime	16 sec
Specific impulse at sea level	214.0 sec
Total impulse at sea level	55,600 lb-sec

a. (S) The canard control fins, located well forward, cause rapid reaction to control fin deflection. An advantage of canard configuration is that the lift due to control deflection and resulting angle of attack of the missile are additive. The 45 degree orientation provides an increase in control effectiveness over an alignment of the fins in the pitch and yaw planes. Calculations show control effectiveness probably would be marginal at altitudes of about 35,000 feet due to low dynamic pressure and the relatively small control fin area. (See Appendix II.)

b. (S) The clipped-delta stabilizer fins are attached to the sustainer motor section. Small fixed tabs, probably trim tabs, are attached to the trailing edge of two opposite stabilizer fins. Aileron roll stabilization surfaces are located on the trailing portion of the other two fins. Mechanical control linkages extend the length of the stabilizer fins from the aileron surfaces forward into the guidance section.

c. (S) Rectangular stabilizer fins are hinged to the booster motor case and are folded forward on the missiles. A pressure or hydraulic device appears to operate in conjunction with the hinge mechanism probably to insure proper fin "fold-out" (Figure 16). A locking device located on the root chord of each of the booster stabilizer fins, about two-thirds of the fin width from the hinge point, clamps to the rear of the booster nozzle skirt. In flight position, about one-third of the fin extends beyond the booster nozzle.

2. (S) Boat-tailing has been used on the booster to reduce drag. The sweep-back of the sustainer stabilizer fins indicates probable optimization of the lift-to-drag ratio, and body wave drag is reduced because of the long, tapered, forward portion of the sustainer. The rearward center of pressure shift for the tapered body, as compared to a near cylindrical body reduces the body-alone destabilizing moment and improves control fin effectiveness. The drag reduction techniques and apparent control effectiveness indicate a low-altitude intercept design capability.

3. (S) The additive effect of lift due to control fin deflection and the resulting angle of attack would produce large aerodynamic loads on the GOA sustainer. The allowable loads are dependent on internal missile structure factors which cannot be determined. A design maximum allowable lateral acceleration of about 8 g's appears reasonable, based on fin thicknesses and the fin attachments to the missile body.

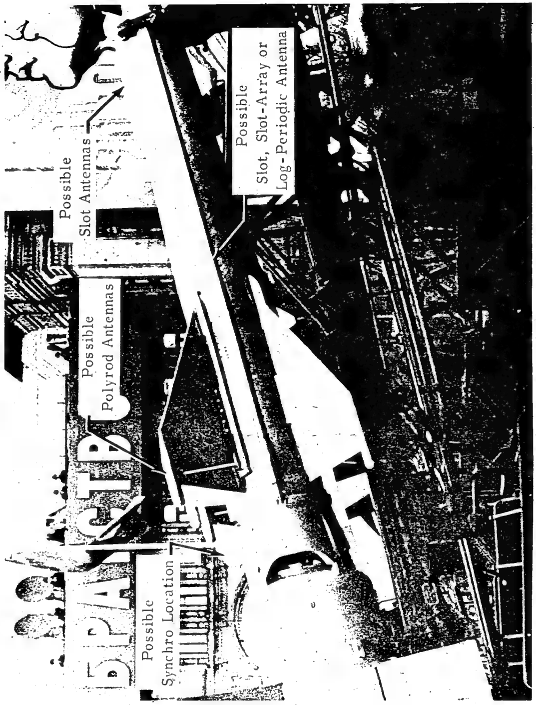

Figure 9. (C) Possible Antenna Locations on the GOA Missile. (U)

4. (S) Examination of similar missile configurations indicates the pitching moment would be nonlinear at 10 to 12 degree angles of attack. The GOA configuration would be difficult to trim to this or higher angle of attack values.

5. (S) A single gyro and the aileron roll stabilizers would be sufficient to sense and counteract any cross-coupled rolling moments induced by a combined pitch and yaw maneuver.

D. (S) Electronics (U)

(S) There are four probable and three possible antennas that can be seen on the GOA sustainer (Figure 9). The four probable antennas, apparently polyrod type, are on the tip of each of the stabilizer fins. A possible slotted-type antenna may be present in the tunnel on the top of the sustainer. The three openings in the tunnel on the side of the sustainer may be antennas. The probable and possible antennas have been examined for indications of the guidance scheme and ground-based electronic portions of the SA-3 missile system.

1. (S) Antennas (U)

a. (S) The four identical antennas located on each of the four stabilizer fin tips appear to be of the polyrod type. Analysis based on scalings indicates a frequency range from 2.4 to 3.0 gigacycles, a bandwidth of about 57°, a gain of 10 db, and a front-to-back ratio of 20 db. At the center frequency of approximately 2.7 gigacycles, the side lobe level should be less than 10 percent of the main beam.

b. (S) The tunnel on top of the forward portion of the sustainer could contain a slotted-type or fuse antenna as well as cabling to by-pass the warhead section.

c. (S) The three openings in the central portion of the tunnels on either side of the sustainer body were examined for an antenna function. A slot-array or log-periodic-type antenna could be fitted in these openings. It cannot be determined from the available photography whether antennas are contained in either the side tunnels or the top tunnel on the sustainer section.

d. (S) See Appendix V for a discussion of a beam rider guidance scheme. (Since a command guidance scheme is more commonly understood, only the beam rider method is discussed in Appendix V.)

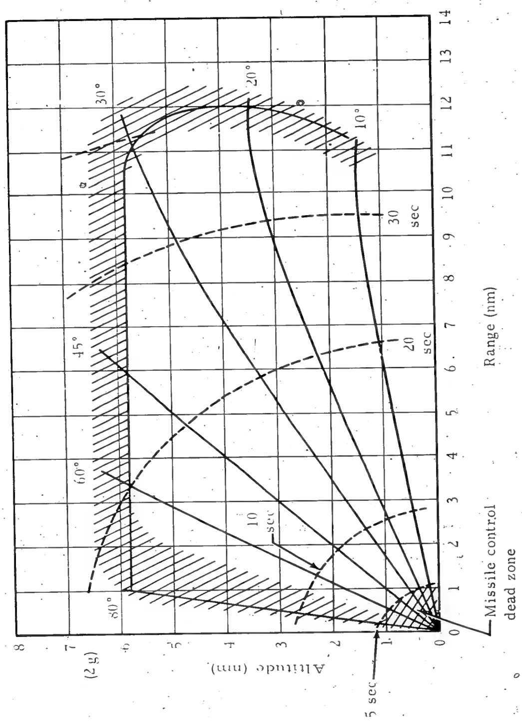

Figure 10. (S) Probable Operating Envelope of GOA Missile. (U)

2. (S) Guidance (U)

a. (S) Command guidance may be used with this missile. If this type guidance is used, two of the polyrod antennas would be used for reception of command signals and the other two would be used for beacon transmission. This guidance system would be similar to the technique used with the SA-2 system.

b. (S) The four polyrod antennas appear to be identical. This suggests that a second type (beam rider) guidance may be employed with the SA-3 missile system. The beam rider system would consist of a target track radar, missile guidance radar and a missile. Both antennas would be contained on the single pedestal of the LOW BLOW radar. The target track radar would acquire and track the target; and, based upon information from this radar, a launching time for the missile would be determined. After launching, the missile would derive its guidance signals from a conically scanned beam being transmitted by the missile guidance radar. The four polyrod antennas would, in this case, receive only.

E. (S) Performance (U)

1. (S) The estimated performance envelope for the GOA missile is shown in Figure 10. Maximum altitude and range capabilities were computed based on assumed minimum control requirements of a 2 g lateral maneuver and a residual speed of Mach 1.3. The performance envelope was obtained by varying the launch angle through a range of 10 to 80 degrees and continuing the missile flight on nonmaneuvering, zero-lift trajectories. A missile control dead zone of 5 seconds is assumed; approximately 4 seconds to booster burnout and 1 second for separation and establishment of guidance control. Target gaming was not considered in this analysis. A better knowledge of the capabilities and limitations of the ground based electronics and target gaming would be required to establish, with reasonable confidence, the intercept capabilities of the system against the various aircraft speeds and flight profiles that would be encountered.

2. (S) The system minimum-altitude capabilities are dependent on the presently unknown characteristics and limitations of the fire control radar. The configuration and characteristics of the GOA missile do not appear to limit the low altitude capabilities of the system (beyond any missile control dead zone).

3. (S) The maximum allowable aerodynamic loads on the GOA sustainer are dependent on unknown internal structure factors.

TABLE 4

(U) ZIL-157 TRUCK CHARACTERISTICS. (U)

Weight	12,000 lb
Payload	
Road	9,900 lb
Cross country	5,500 lb
Towed load	7,920 lb
Length overall	22 ft
Height overall	7.7 ft
Width overall	7.7 ft
Engine	109 HP, 6 Cyl., gasoline
Wheelbase	13.8 ft
Type of drive	6 × 6
Tire size	12.00 × 18
Turning radius	36.8 ft
Cruising range	250 miles
Maximum speed	40 mph
Ground clearance	1.0 ft

Control and stabilizer fin thicknesses, the means used to attach the fins to the body, and the general appearance of the missile indicate a reasonable maximum lateral loading of about 8 g's. A limit of 8 g's has been used to compute the maximum allowable angle of attack as a function of altitude, Mach number, and control fin deflection angle (Appendix II). The maximum control fin deflection angle is also unknown; however, an apparently reasonable value of 15 degrees was assumed for the computations.

F. (S) Warhead (U)

1. (S) The location of the warhead section (under the top tunnel on the missile) was determined by pictorial analysis. The diameter and length of the warhead section would accommodate a 200 pound warhead kit, or a 175 pound warhead.

2. (S) The GOA missile warhead is probably a high explosive, directional fragmentation type. No estimate of the lethal radius or the fragmentation pattern is included in this analysis.

G. (S) Transporter (U)

1. (S) General (U)

(S) The GOA missile transporter utilizes the ZIL-157 truck as the basic vehicle. The transporter provides a means of checking out and servicing the missiles, loading of the launcher, and missile storage prior to site replenishment. The estimated weight of a fully loaded transporter is about 18,000 pounds divided as follows:

Missile (each)	2000 lb
Ordnance equipment	2000 lb
ZIL-157 truck	12,000 lb

2. (C) ZIL-157 Truck (U)

(C) The transporter mechanism is mounted on the chassis of the standard 6 × 6 ZIL-157 truck. Many features of the basic vehicle closely resembly the U.S. World War II $2\frac{1}{2}$ ton, 6 × 6, truck. Characteristics of the vehicle are shown in Table 4.

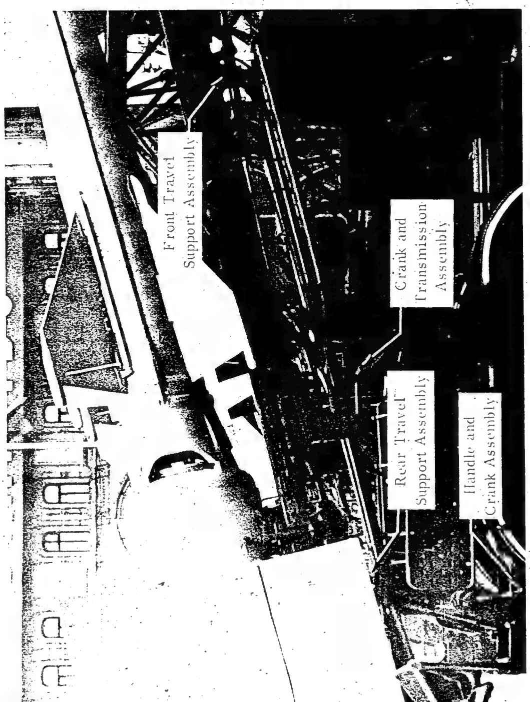

Figure 11. (C) Main Support Beam Mounting Points. (U)

3. (S) Transport and Loading Mechanisms (U)

a. (S) The transport and loading mechanism is a dual beam arrangement with each beam supporting one missile. Each beam is attached to the truck chassis at two points. The forward support is a pivot point and the rear support is an elevating mechanism (Figure 11).

b. (S) The elevating mechanism permits raising the rear portion of the beam to mate with rails on the missile launcher. The beams are probably capable of being elevated independently. The elevating mechanism appears to be operated by a hand crank.

c. (S) Each missile is supported on its beam by a forward "C" clamp and rear cradle (Figure 12). A hand crank and transmission assembly on the under side of each beam is connected to a chain drive to load and off-load the missile (Figure 11). A large handle above the gear box (with arrows) is a braking/gear shift mechanism used in conjunction with the loading power train. Figure 13 shows the concept of the loading assembly.

d. (S) The forward support assembly (C-clamp), in the travel position, is tied down to the main beam at three points (Figure 14). A small hand screw just under the missile body is used to hold the forward support assembly against a bracket fixed to the main beam. Two T-bar clamps, one on either side, tie down the forward support assembly to the main beam to prevent lateral motion. A small hand screw, just below the T-bars, permits release of the T-bar clamps by an "up-and-out" motion. A grip release is used to release the C-clamp from the missile.

e. (S) The missile booster is tied down to the main beam in the travel position by two turn-buckle-type clamps, one on either side, opposite the rear support assembly or cradle (Figure 15).

f. (S) Two small probable fire-proof switch boxes and flood lights are located at the main tie-down points of the missile and at the rear end of the missile support beam, providing necessary light for operation in areas where general illumination is not available or cannot be used (Figures 14 and 15).

4. (S) Missile Checkout and Servicing Equipment (U)

a. (S) A probable umbilical connector for preliminary missile checkout is mounted on the outside of each of the missile support

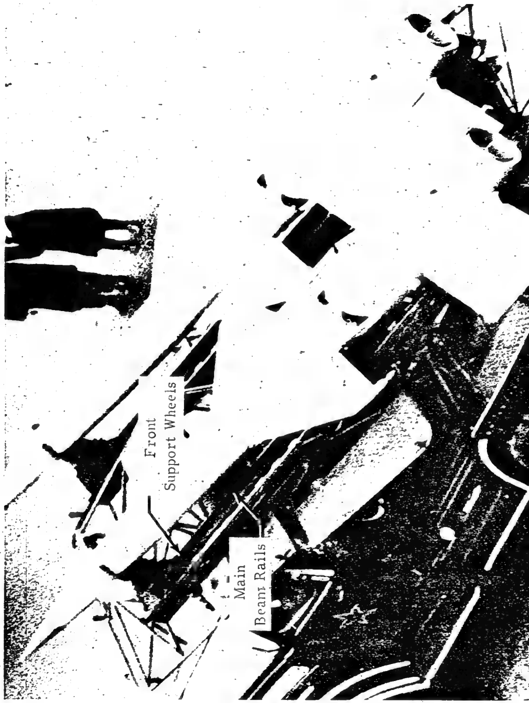

Figure 12. (C) GOA Missile Transporter. (U)

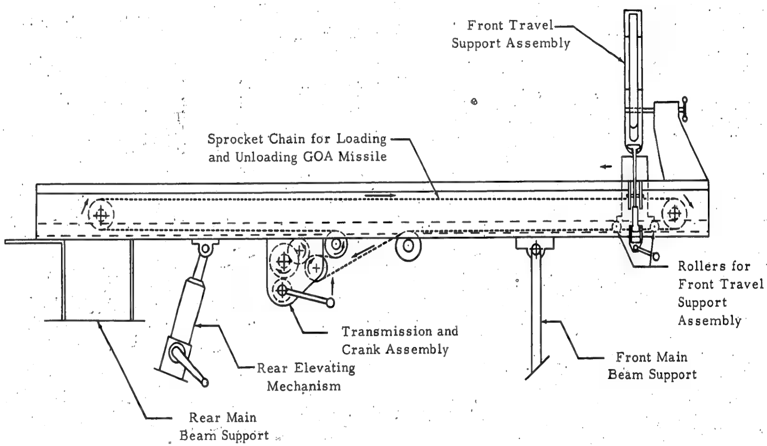

Figure 13. (C) Geometry of the Loading and Unloading Transmission Assembly. (U)

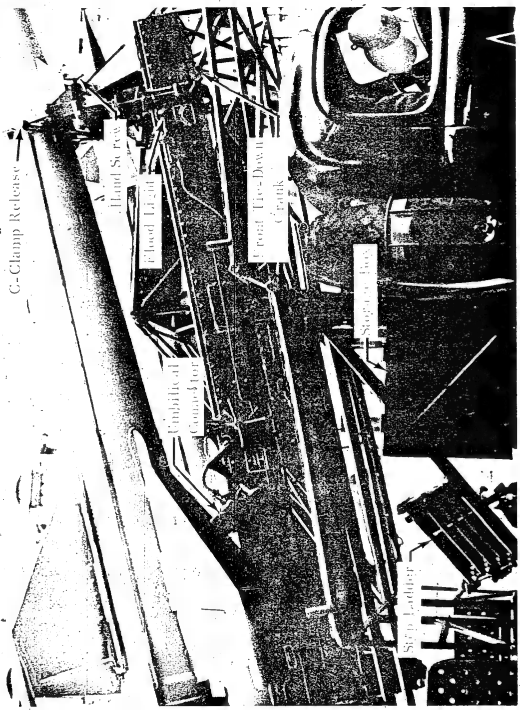

Figure 14. (C) Front Support Assembly. (U)

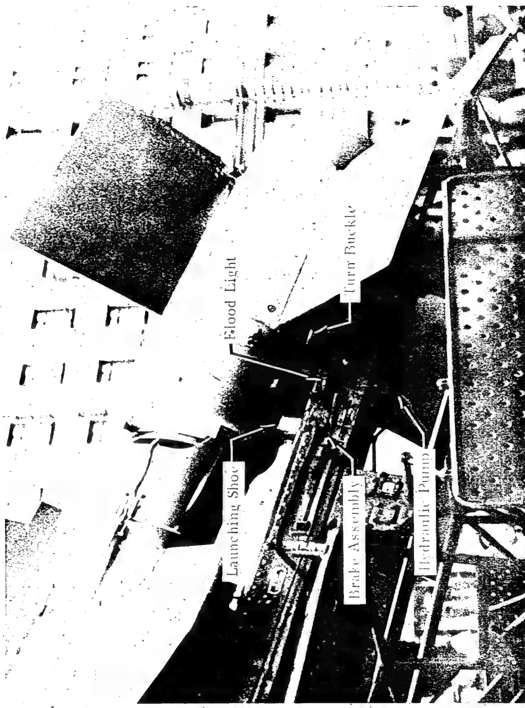

Figure 15. (C) Loading and Unloading Brake Mechanism. (U)

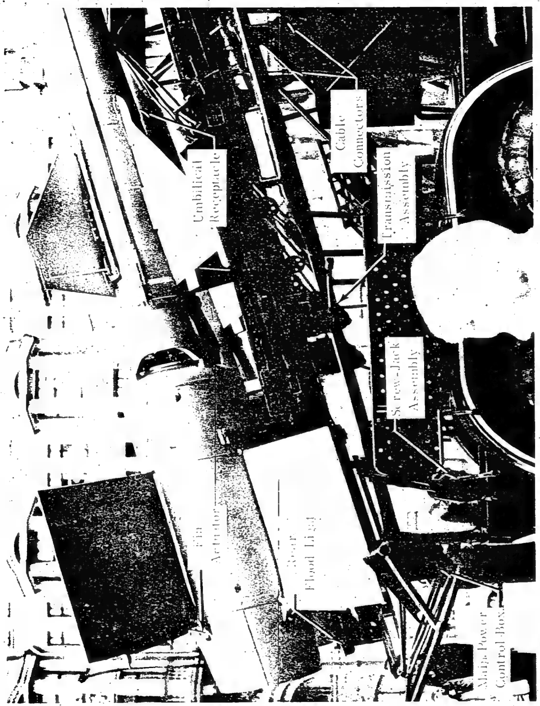

Figure 16. (C) GOA Transporter Main Beam Assembly. (U)

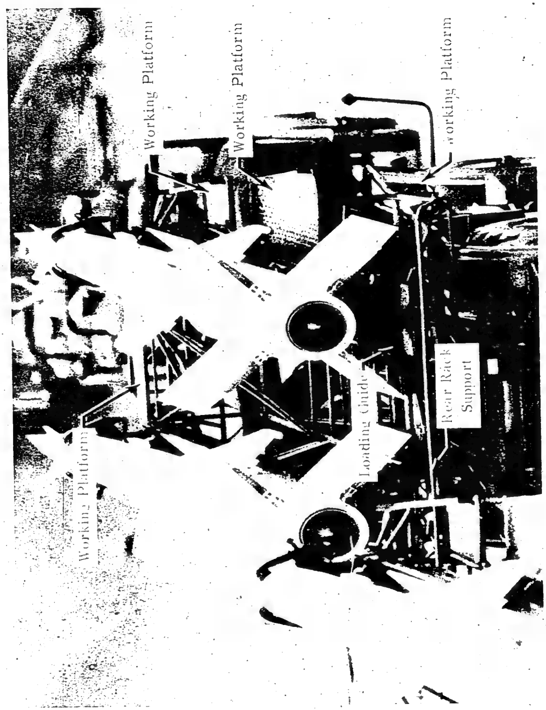

Figure 17. (C) Recognition Features of the GOA Transporter. (U)

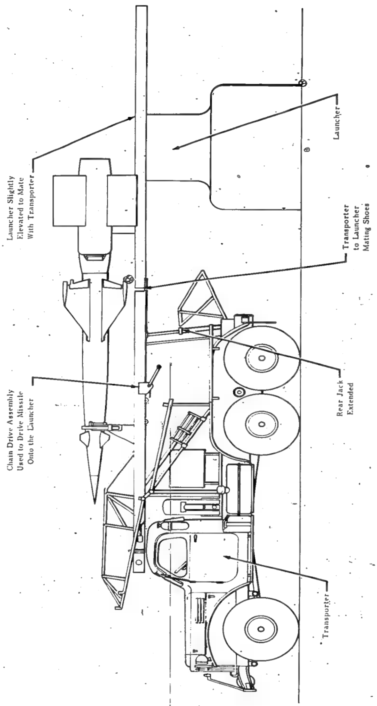

Figure 18. (C) GOA Loading Profile Onto the Launcher. (U)

beams (Figure 14). The connector box, mounted on a three-jointed rod, rotates upward and inward to permit contact with the under side of the missile at the rear portion of the guidance and control compartment.

b. (S) Hydraulic power for missile checkout is probably provided by a hydraulic pump on the underside of the main beam (Figure 15). Several small high pressure tubes can be observed leading into or out of this location.

c. (S) The box on the right side of the vehicle just behind the spare tire rack probably provides storage space for tools and cables used in the missile checkout procedure (Figure 14). A small box at the rear of the vehicle between the missile support beams probably contains cable connectors for external checkout control and power (Figure 16).

d. (S) The welded tubular framework fixed to the vehicle supports provides working platforms for easy access to all parts of both missiles and the missile loading mechanism and provides brush-guard type protection for the missiles (Figure 17). Stanchions are provided for bows to add overhead protection and to support a tarpaulin-type cover.

5. (S) <u>Transfer of Missiles from Transporter to Launcher</u> (U)

a. (S) Figure 18 depicts a concept of a possible mating of the transporter to the launcher for transloading operations.

b. (S) A rail rather than a zero-length launch system is probable. The missiles are apparently rolled back along the transporter missile support beam onto the launcher rails rather than lifted and placed as would be necessary with a zero-length system.

c. (S) A thick, horseshoe-shaped object is welded to the bottom of the booster case (Figure 15) and, although the lower part of the object is hidden from view by the missile support beam, the size and location of the object make it a principal candidate for a shoe-slide or roller-type attachment with the launch rail (Figure 15). There is no forward attachment point visible on the missile but one probably exists. A cantilevered-type missile support at one point on the launch rail is possible but unlikely. The moment resulting from booster thrust would be high and elaborate methods would be necessary to prevent binding.

d. (S) Transloading is probably a manual operation as indicated by the transporter. Missile support beam elevation, tie-down disconnects, and transloading mechanisms are operated by hand cranks and wheels. Electrically or hydraulically powered equipment features are not visible on the transporter.

APPENDIX I. (S) GOA MISSILE PROPULSION ANALYSIS (U)

1. (U) Notation (U)

A_e nozzle exit area

A_p propellant surface area

A_t nozzle throat area

a burning rate constant

c effective exhaust velocity

c^* characteristic exhaust velocity

C_d nozzle discharge coefficient = 1

C_f thrust coefficient

c_p specific heat at constant pressure

c_v specific heat at constant volume

F thrust

g gravitational acceleration

I_{sp} specific impulse

K ratio of propellant surface area to nozzle throat area

k ratio of gas specific heats = 1.23

M molecular weight of gases

n burning rate pressure exponent

P_a ambient pressure

P_c chamber pressure

P_e nozzle exit pressure

R gas constant

r propellant burning rate

T_c chamber temperature

t_b burntime

V_c chamber volume

V_p propellant volume

W_p total propellant weight

$\dot{w}$ weight flow rate of propellant

(U) Greek Symbols (U)

π_k sensitivity of burning rate to temperature at constant K

π_p sensitivity of burning rate to temperature at constant chamber pressure

ρ_p propellant density

Ω function of k alone

ω ratio of chamber volume to propellant volume

(U) Subscripts (U)

a ambient

c chamber

e exit

sl sea level

t throat

vac vacuum

2. (U) Equations (U)

Thrust

$$F = P_c A_t C_f$$

$$= I_{sp} \dot{w}$$

$$= \mathring{A}_p r \rho_p I_{sp}$$

$$= \frac{c\dot{w}}{g}$$

Thrust Coefficient

$$C_f = \sqrt{\frac{2k^2}{k-1}\left(\frac{2}{k+1}\right)^{\frac{k+1}{k-1}}\left(1 - \frac{P_e}{P_c}^{\frac{k-1}{k}}\right)} + \frac{P_e - P_a}{P_c}\left(\frac{A_e}{A_t}\right)$$

Chamber Pressure

$$P_c = \frac{\dot{w}\sqrt{T_c/M}}{0.1443\, C_d\, A_t\, \Omega}$$

$$P_c \sim \left(\frac{A_p}{A_t}\right)^{\frac{1}{1-n}} = K^{\frac{1}{1-n}}$$

Nozzle Area Ratio

$$\frac{A_e}{A_t} = \frac{\left(\frac{2}{k+1}\right)^{\frac{1}{k-1}}\left(\frac{P_c}{P_e}\right)^{\frac{1}{k}}}{\sqrt{\left(\frac{k+1}{k-1}\right)\left(1 - \frac{P_e}{P_c}^{\frac{k-1}{k}}\right)}}$$

Propellant Surface to Throat Area Ratio

$$\frac{A_p}{A_t} = K = \frac{P_c \sqrt{g k \left(\frac{2}{k+1}\right)^{\frac{k+1}{k-1}}}}{\rho_p \, r \sqrt{R \, T_c}}$$

Propellant Volume

$$V_p = \frac{W_p}{\rho_p}$$

$$= \frac{F \, t_b \, g}{\rho_p \, C}$$

$$= \frac{V_c}{\omega}$$

Burning Rate

$$r = a \, P_c^{\;n}$$

Volume Ratio

$$\omega = \frac{V_c}{V_p}$$

Weight Flow

$$\dot{w} = \frac{W_p}{t_b}$$

$$= \frac{F}{I_{sp}}$$

$$= \frac{P_c (0.4443) \, C_d \, A_t \, \Omega}{\sqrt{T_c / M}}$$

$$= A_p \, r \, \rho_p$$

Propellant Density

$$\rho_p = \frac{W_p}{V_p}$$

General

$$\Omega = \sqrt{k}\left(\frac{2}{k+1}\right)^{\frac{k+1}{2(k-1)}}$$

$$k = \frac{c_p}{c_v}$$

Specific Impulse

$$I_{sp} = \frac{F}{\dot{w}}$$

$$= \frac{c}{g}$$

$$= \frac{C_f c^*}{g}$$

Effective Exhaust Velocity

$$c = \sqrt{\frac{2gk}{k-1} R T_c \left(1 - \frac{P_e}{P_c}^{\frac{k-1}{k}}\right)} + \frac{(P_e - P_a) A_e g}{\dot{w}}$$

Characteristic Exhaust Velocity

$$c^* = \frac{P_c A_t g}{\dot{w}}$$

$$= \frac{I_{sp} g}{C_f}$$

$$c^* = \frac{\sqrt{g k R T_c}}{\sqrt{2\left(\frac{2}{k+1}\right)^{\frac{2}{k-1}}\left(\frac{k^2}{k+1}\right)}}$$

3. (S) Booster Propulsion Analysis (U)

a. (S) Observable externals of the GOA missile booster propulsion system indicate a standard solid propellant rocket motor, probably similar in design concept to the GUIDELINE (SA-2) booster. Major components are a cylindrical motor case with ellipsoidal ends, a probable electrically actuated igniter, solid propellant grain, a converging-diverging nozzle, and a nozzle plug.

b. (S) A dimensional analysis was performed on the booster (Figure 19). The dimensions used in estimating motor performance and component weights are:

Nozzle exit diameter	12.99 in
Nozzle exit area	132.5 in^2
Outside diameter of case	21.26 in
Case length (estimated)	53 in
Motor length	68.6 in

c. (S) The motor case was assumed to be steel based on the types and locations of welds, end closure configuration, and the probable range of combustion chamber pressures and temperatures. The Soviets published military-type specifications in 1957 for chromium, vanadium steel for "rocket motors and casings". This steel, designated EI-659, is a ductile structural type capable of heat treatment after welding and highly suited to machine welding (for thickness greater than 3 mm). EI-659 has an ultimate stress of about 170,000 psi and a yield stress of 85,000 to 90,000 psi. Standard Soviet practice would permit a design stress of 45,000 to 50,000 psi. A design hoop stress of 50,000 psi and a chamber pressure of 1250 psia would require a case wall thickness of approximately 0.276 inches (7 mm). The width of the machine-made weld seams is compatible with a wall thickness of approximately 0.24 to 0.32 inches (6 - 8 mm), or thicker.

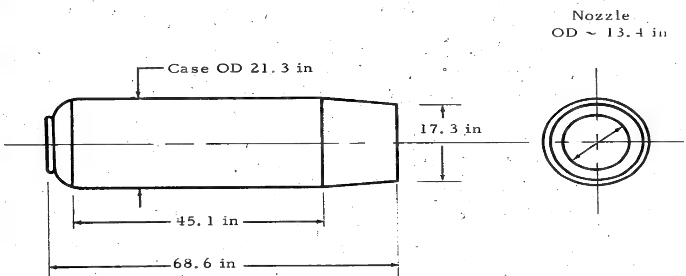

Figure 19. (S) Booster Motor Envelope. (U)

d. (S) An insulating motor case liner would be required to prevent overheating the walls. An insulation thickness of about 0.1 inch would limit wall temperatures to about 600°F. A throat liner of corundum is probably utilized to prevent hot gas erosion.

e. (S) The configuration similarity of the GOA booster to the GUIDELINE booster suggests that the propellants are probably similar. The design period for the GOA missile probably followed that for the GUIDELINE by not more than one to two years. The assumption that the booster propellants are identical provides a good approximation of the GOA booster performance characteristics. An extruded double-base solid propellant, identical to that used in the SA-2, is used for calculation of booster performance. Eight propellant sticks, 5.71 inches in diameter and 48 inches long, can be placed in the motor case (Figures 8 and 20). Propellant grain supports would be required to separate the propellant sticks.

(1) (S) Propellant characteristics are believed to be similar to a U.S. double-base type designated OV and listed in the Propellant Powder Manual as unit 137 (developed by Allegheny Ballistics Laboratory for JATO use). The estimated characteristics of the GOA booster propellant, used for calculation of probable booster performance, are summarized as follows:

Stick dimensions (each)

- OD - 5.71 in
- ID - 1.417 in
- Web - 2.147 in
- Length - 48 in

Density - 0.0564 lb/in^3

Ratio of specific heats (k) - 1.23

Molecular weight of gases - 26.8

Combustion temperature - 4290°R

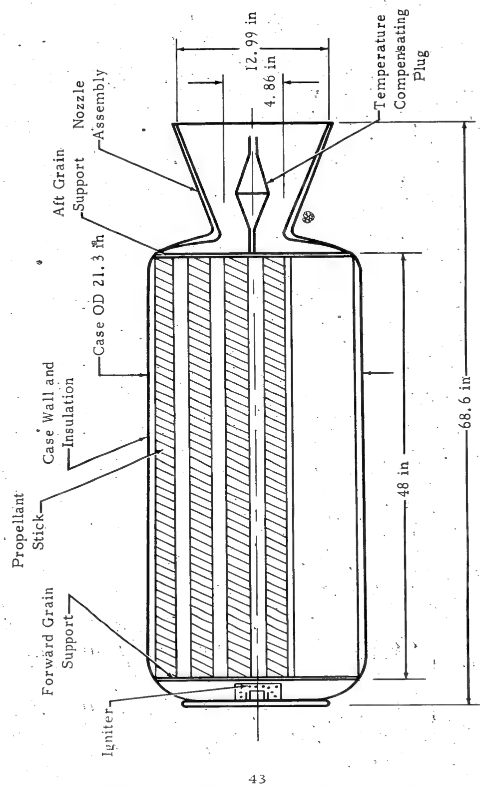

Figure 20. (S) Assumed Booster Motor Configuration. (U)

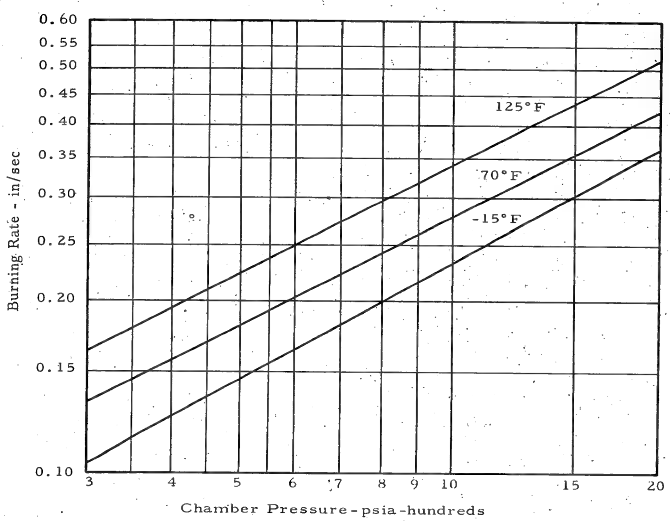

Figure 21. (S) Estimated Burning Rate as a Function of Chamber Pressure for Several Propellant Temperatures. (U)

(2) (S) The propellant volume, based on 8 sticks of the assumed dimensions, would be 9165 in^3 and the weight would be 517 pounds. The combustion chamber volume is about 14,650 in^3 and the propellant loading factor is then 59 percent.

(3) (S) Burning rate (r) of the propellant is presented in Figure 21 as a function of propellant temperature and combustion chamber pressure (P_c).

f. (S) A combustion chamber pressure of 1200 psia was assumed for computations of booster performance characteristics. Table 5 presents the booster performance parameters at propellant ambient temperatures of 70°F, -15°F, and 125°F.

(1) (S) In this analysis, the nozzle plug was assumed to be adjusted to maintain a constant chamber pressure of 1200 psia over the range of propellant grain temperatures. Such use of the nozzle plug would partially compensate for variations in propellant temperatures but would not eliminate variations in thrust and burntime.

(2) (S) The nozzle plug could be used to maintain essentially the same thrust and burntime regardless of the propellant temperature but this use would be accompanied by an increase in chamber pressure of about 25 percent for low ambient temperature conditions. This increase in pressure would require a proportionate increase in case wall thickness and weight.

4. (S) Sustainer Propulsion Analysis (U)

a. (S) The external appearance of the sustainer motor section and the absence of fill plugs and access hatches is suggestive of a standard solid propellant rocket motor. Major components are a standard cylindrical motor, probably with ellipsoidal ends, solid propellant grain, a probable standard electrically actuated igniter, converging-diverging nozzle, and probably a nozzle plug (Figure 22).

b. (S) The dimensions used in estimating sustainer motor performance and component weights are:

Nozzle exit diameter	5.34 in
Nozzle exit area	22.47 in^2

TABLE 5

(S) BOOSTER PERFORMANCE. (U)

	-15°F	70°F	125°F
Propellant wt. (lbs)	517	517	517
Chamber pressure (psia)	1200	1200	1200
Burning rate (in/sec)	0.258	0.295	0.359
Flow rate (lb/sec)	124.27	142.09	172.91
Nozzle throat area (in^2)	13.785	15.865	19.306
Nozzle exit area (in^2)	132.5	132.5	132.5
Expansion ratio	9.5495	8.3517	6.8632
Nozzle pressure ratio	0.01230	0.01478	0.01930
Nozzle exit pressure (psia)	14.8	17.7	23.2
Thrust coefficient at sea level	1.6026	1.6011	1.5943
Thrust at sea level (lbs)	26,680	30,480	36,940
Specific impulse at sea level (sec)	214.7	214.5	213.6
Burntime (sec)	4.16	3.64	2.99
Total impulse at sea level (lb-sec)	111,000	110,897	110,431
Cross sectional loading (%)	53.2	53.2	53.2
Assumed mass fraction	0.62	0.62	0.62
Motor weight (lbs)	834	834	834
Assumed thrust correction factor	1.0	1.0	1.0

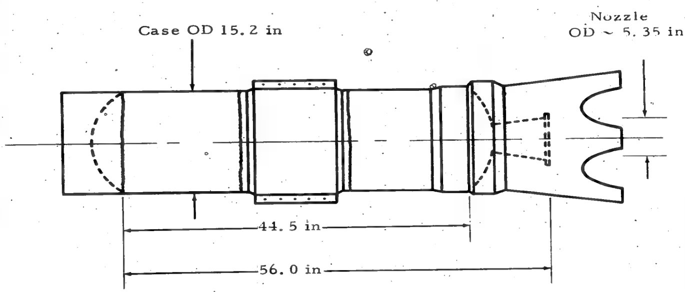

Figure 22. (S) Sustainer Motor Envelope. (U)

Outside diameter of case	15.2 in
Case length (estimated)	51.14 in
Motor length (estimated)	59.62 in

c. (S) The motor case material was assumed to be steel of the same type assumed for the booster. A case thickness of about 0.197 inches (5 mm) would be required. An insulation material thickness of about 0.1 inch was also assumed.

d. (S) The propellant used in the sustainer motor is probably the same double-base type as that assumed for the booster. The grain type would be changed to provide a lower thrust level for a longer duration. Several assumptions are necessary to arrive at a reasonable motor estimate.

(1) (S) Chamber pressures for the lower and upper combustion limits for a double-base propellant would be about 400 psia and 2500 psia, respectively. Combustion stability becomes a problem near these limits, particularly with substantial variations in ambient grain temperature, and reliability would be adversely affected. Soviet practices stress reliability, therefore, more reasonable chamber pressure limits would be from 1000 to 2000 psia. A chamber pressure of 1200 psia has been assumed for computations in this study.

(2) (S) Various thrust levels and burntimes for the sustainer motor were investigated to determine the overall effects on missile performance. Based upon the probable sustainer propellant weight and chamber pressure, a near optimum performance would occur with a thrust and burntime of 3477 pounds and 16 seconds, respectively.

(3) (S) The assumed chamber pressure and burntime would require an internal burning grain. The time consuming and involved process of designing a grain to fit all the parameters was not attempted. There are many solutions that would provide the necessary performance for the sustainer. The assumed values for the propellant volume, weight, and surface area are:

Volume (V_p)	4610 in^3
Weight (W_p)	260 lb
Surface area (A_p)	977 in^2

e. (S) Sustainer performance values were calculated for ambient powder temperatures of 70°, -15°, and 125°F and are listed in Table 6.

TABLE 6

(S) SUSTAINER PERFORMANCE. (U)

	-15°F	70°F	125°F
Propellant weight (lbs)	260	260	260
Chamber pressure (psia)	1200	1200	1200
Burning rate (in/sec)	0.258	0.295	0.359
Flow rate (lb/sec)	14.21	16.25	19.78
Nozzle throat area (in^2)	1.59	1.81	2.21
Nozzle exit area (in^2)	22.47	22.47	22.47
Expansion ratio	14.161	12.385	10.177
Nozzle pressure ratio	0.0073	0.0087	0.0113
Nozzle exit pressure	8.72	10.4	13.57
Thrust coefficient at sea level	1.589	1.597	1.602
Thrust at sea level (lbs)	3026	3477	4245
Specific impulse at sea level (sec)	212.9	214.0	214.7
Burntime (sec)	18.3	16.0	13.2
Total impulse at sea level (lb-sec)	55,354	55,632	55,822
Assumed mass fraction	0.52	0.52	0.52
Motor weight (lb)	500	500	500
Assumed thrust correction factor	1.0	1.0	1.0

APPENDIX II. (S) MISSILE AERODYNAMICS (U)

A. (U) Symbols and Nomenclature (U)

(U) The aerodynamic forces, moments, and angles are referred to the body-axis system (Figure 23). The following symbols and nomenclature are used throughout this report:

Notation:

α	Angle of attack: angle between the missile velocity vector and missile longitudinal axis	degrees
γ	Missile flight path angle: angle between the local horizontal and missile velocity vector	degrees
δ	Control fin deflection angle: angle between the missile longitudinal axis and the long axis of the control fin, measured in the plane containing the missile longitudinal axis and perpendicular to the control fin transverse axis	degrees
θ	Missile attitude angle: angle between the local horizontal and the missile longitudinal axis	degrees
ρ_∞	Ambient air density	slugs/ft^3
A	Axial force	pounds
C_A	Axial force coefficient ($C_A = A/q\,s$)	
C_D	Drag force coefficient ($C_D = D/q\,s$)	
C_L	Lift force coefficient ($C_L = L/q\,s$)	
C_M	Pitching moment coefficient ($C_M = M/q\,s\,d$)	
$C_{M\alpha}$	Rate of change of pitching moment coefficient with respect to angle of attack	per degree

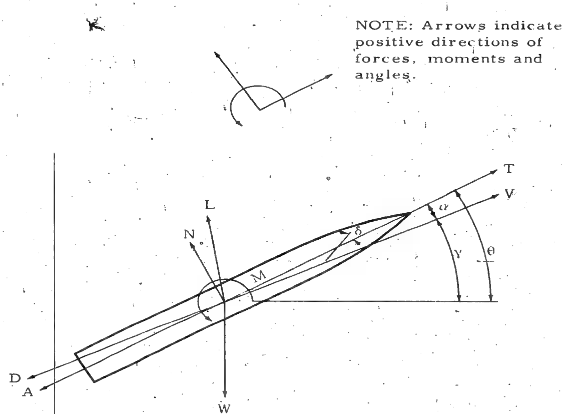

Figure 23. (U) Nomenclature and Sign Convention. (U)

$C_{M\delta}$	Rate of change of pitching moment coefficient with respect to control fin deflection angle	per degree
C_N	Normal force coefficient ($C_N = N/q\,s$)	
$C_{N\alpha}$	Rate of change of normal force coefficient with respect to angle of attack	per degree
$C_{N\delta}$	Rate of change of normal force coefficient with respect to control fin deflection angle	per degree
D	Drag force	pounds
d	Diameter	feet
f	Fineness ratio (ℓ/d)	
k	Ratio of specific heats for air ($k = 1.4$)	
L	Lift force	pounds
ℓ	Length	feet
M	Pitching moment	ft-lb
M_∞	Free stream Mach number	
N	Normal force	pounds
p_∞	Ambient static pressure	lb/ft^2
q	Dynamic pressure [$q = (p_\infty M_\infty^2)k/2 = (\rho_\infty V_\infty^2)/2$]	lb/ft^2
s	Missile body cross-sectional area [$s = (\pi d^2)/4$]	ft^2
T	Thrust	pounds

V_∞	Free stream velocity	ft/sec
W	Missile weight	pounds
X_{CG}/d	Location of center of gravity in calibers from nose	
X_{CP}/d	Location of center of pressure in calibers from nose	

Subscripts

b	Body
CF	Control fins
BF	Booster stabilizer fins
SF	Sustainer stabilizer fins
t	Total configuration

B. (S) Aerodynamic Analysis (U)

1. (U) Aerodynamic force coefficients and center of pressure locations were calculated considering the contributions of the various aerodynamic components, fin-body interference effects, and the effects of control fin vortices acting in the area of the downstream stabilizer fins.

a. (U) Body Alone Data (U)

(U) The zero-lift wave (form) drag and normal force coefficients and center of pressure locations were determined from slender body theory for subsonic Mach numbers and from second order shock expansion theory for supersonic Mach numbers. The transonic trend for the body-alone data was obtained by comparison with Reference 1. Power-off base drag was obtained by correlation with experimental data (Reference 2). Power-on base drag was determined from an empirical method (Reference 3) based on altitude, thrust and missile geometry.

b. (U) Control and Stabilizer Fin Data (U)

(U) Wave drag and normal force coefficients and center of pressure locations for the control and stabilizer fins were determined using References 4 through 6 for the subsonic, transonic, and supersonic regimes.

c. (U) Skin Friction Drag (U)

(U) The effects of skin friction on the drag of the various aerodynamic components were determined from skin friction charts for an insulated flat plate as a function of Reynolds and Mach numbers (appropriately modified for the bodies of revolution).

d. (U) Aerodynamic Force Coefficients (U)

(U) Variations in the location of the center of pressure with Mach number and for a small range of angle of attack were computed and are shown in Figure 24. Power-on and power-off zero-lift drag coefficients as a function of altitude and Mach number are shown in Figure 25. Figure 26 shows the rate of change of normal force coefficient with respect to angle of attack, C_{N_α}, as a function of Mach number for a small angle of attack range. Additional body and fin data are shown in Figures 27 through 29 for general information.

2. (U) The angle of attack and control fin deflection angle relationship for sustainer trim conditions was investigated for various center of gravity locations. Under steady state (trim) conditions, the summation of the moments about the sustainer center of gravity must be zero. That is

$$C_{M_{CG}} = C_{M_\alpha}\alpha + C_{M_\delta}\delta = 0$$

where

$$C_{M_\alpha} = C_{N_{\alpha_b}} \frac{(X_{CG} - X_{CP_b})}{d} + C_{N_{\alpha_{CF}}} \frac{(X_{CG} - X_{CP_{CF}})}{d} + C_{N_{\alpha_{SF}}} \frac{(X_{CG} - X_{CP_{SF}})}{d}$$

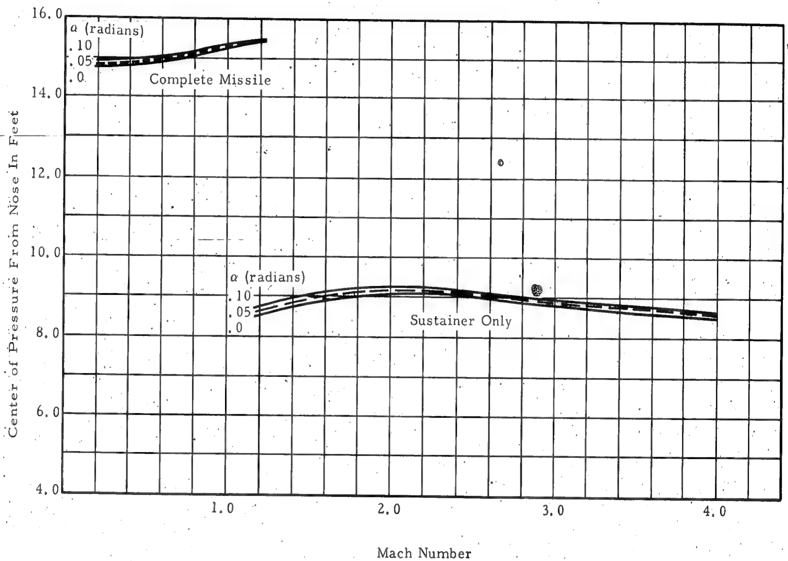

Figure 24. (S) Center of Pressure Location versus Mach Number for Complete Missile and Sustainer. (U)

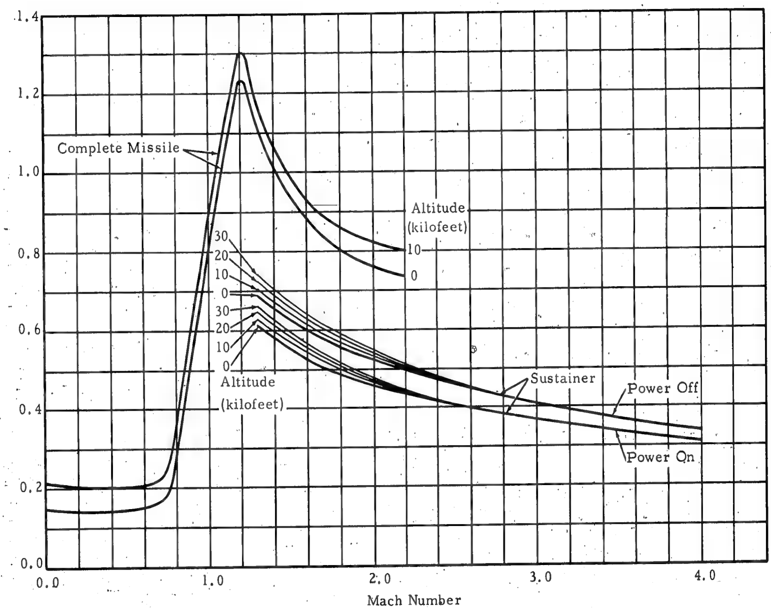

Figure 25. (S) Zero-Lift Drag Coefficient, C_D, as a Function of Mach Number and Altitude. (U)

and

$$C_{M_\delta} = C_{N_{\delta_{CF}}} \frac{(x_{CG} - x_{CP_{CF}})}{d} .$$

The ratio of control fin deflection angle to angle of attack is then

$$\frac{\delta}{\alpha} = - \frac{C_{M_\alpha}}{C_{M_\delta}} .$$

The ratio of δ/α for varying center of gravity locations and Mach number is shown in Figure 30.

3. (S) The total normal force on the GOA missile sustainer per degree angle of attack as a function of Mach number and altitude is shown in Figure 31.

4. (S) The allowable aerodynamic loads on the GOA sustainer are dependent upon unknown internal structure factors. A maximum allowable lateral acceleration of about 8 g's appears reasonable based on fin thickness and the means used to attach the fins to the missile body. The maximum control fin deflection angle is also unknown; a value of 15 degrees appears reasonable and provides adequate performance. A maneuver limit of 8 g's and maximum control deflection angle of 15 degrees were used for a preliminary study of the steady-state angle of attack at various altitudes and Mach numbers.

a. (S) Figures 32 and 33 show the variation of steady state angle of attack (α) and maximum allowable control fin deflection angle (δ), with altitude for sustainer ignition and sustainer burnout. The Mach numbers shown are the estimated maximum and minimum for both ignition and burnout. The assumed maximum load of 8 g's limits the total angle of attack (components in both pitch and yaw planes) up to the assumed 15-degree limit on control fin deflection angle.

b. (S) The sustainer center of gravity moves forward about 10 inches (from 102.4 to 92.2 inches from the nose) while the sustainer motor is burning (Figure 34). The change in moment arms results in decreasing the steady-state (trim) angle of attack for a given control fin deflection angle or, conversely, an increase in

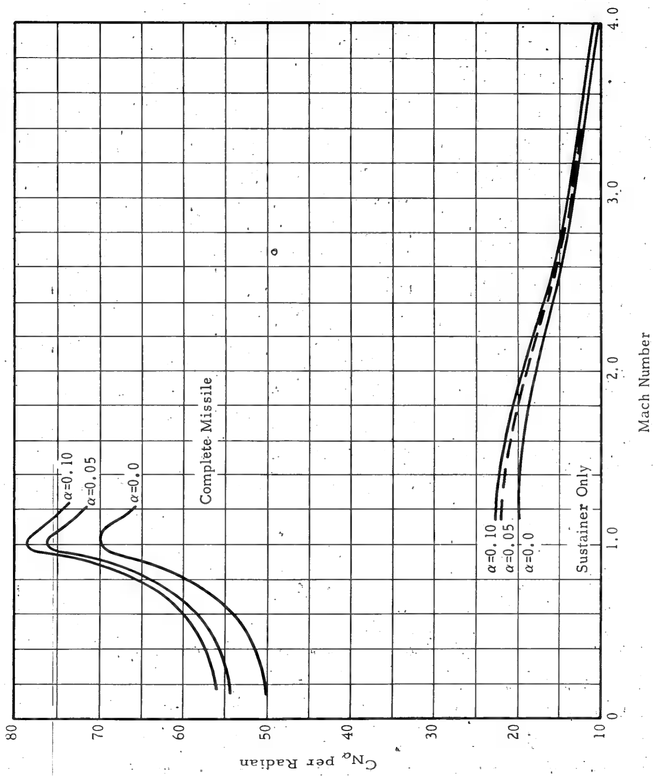

Figure 26. (S) Variation of C_{N_α} with Mach Number. (U)

NOTE: Interference and down-wash effects are included.

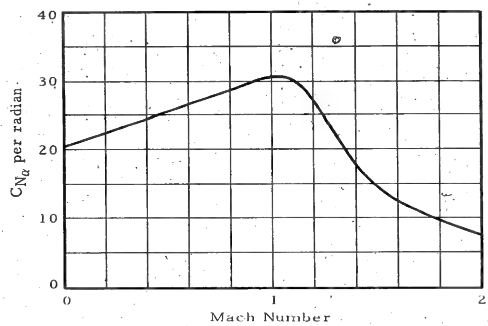

Figure 27. (S) Booster Stabilizer Fins; Variation of C_{N_α} With Mach Number. (U)

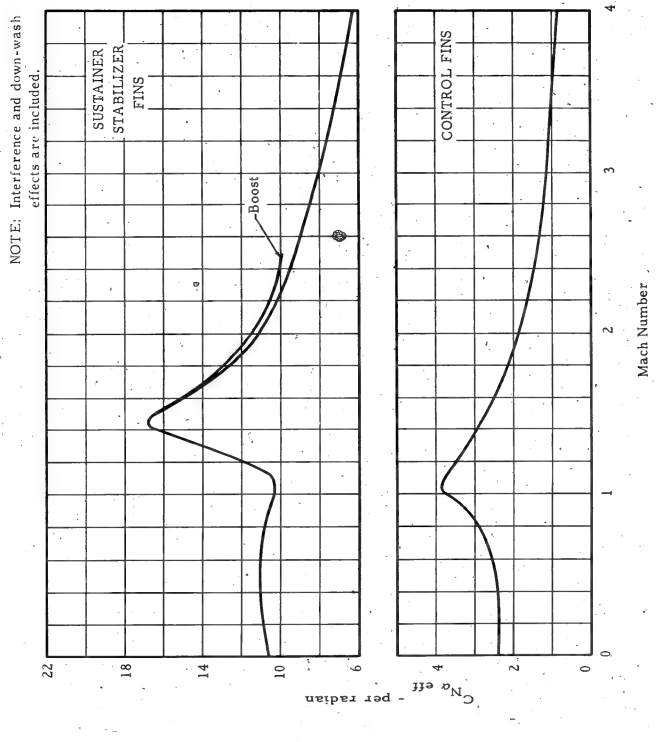

Figure 28. (S) Variation of C_{N_α} with Mach Number, Sustainer Stabilizer and Control Fins. (U)

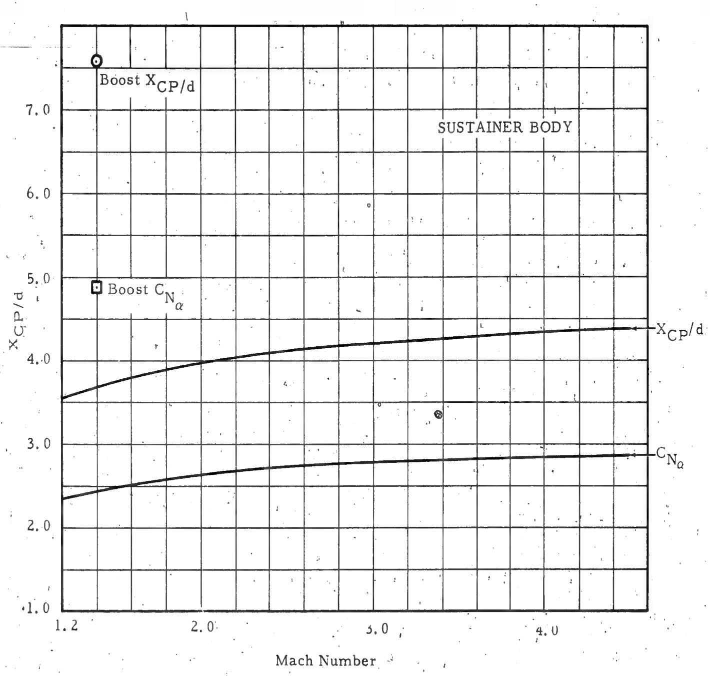

Figure 29. (S) Variation of C_{N_α} and Center of Pressure with Mach Number. (U)

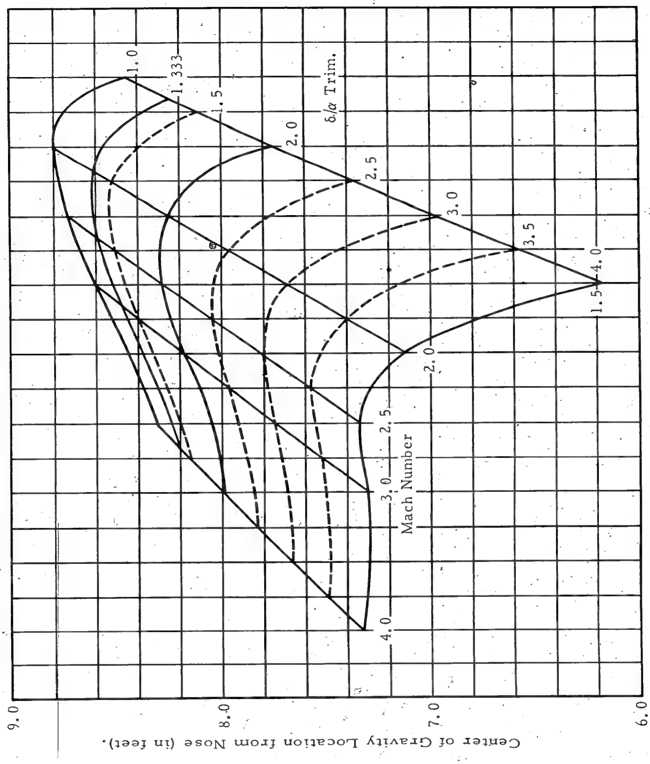

Figure 30. (S) δ/α_{trim} as a Function of Mach Number. (U)

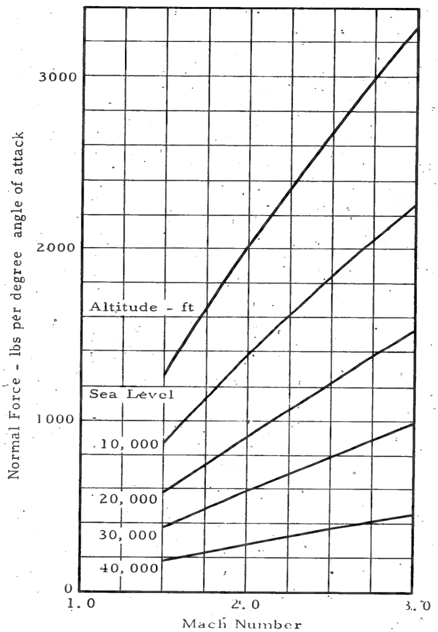

Figure 31. (S) Normal Force per Degree Angle of Attack Variation with Mach Number and Altitude. (U)

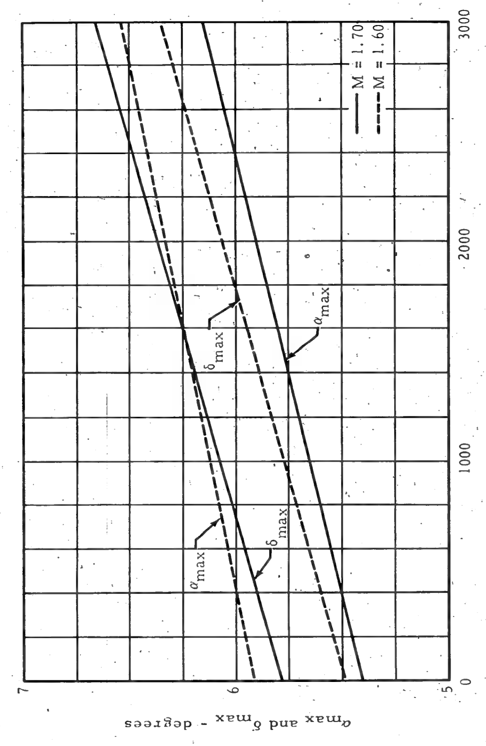

Figure 32. (S) Maximum Allowable α and δ as a Function of Altitude (Sustainer Ignition). (U)

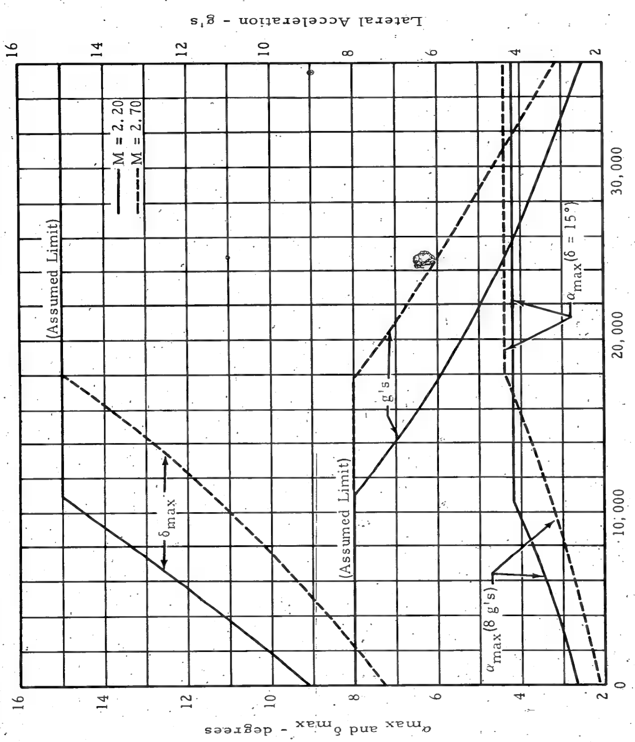

Figure 33. (S) Maximum Allowable α and δ as a Function of Altitude (Sustainer Burnout). (U)

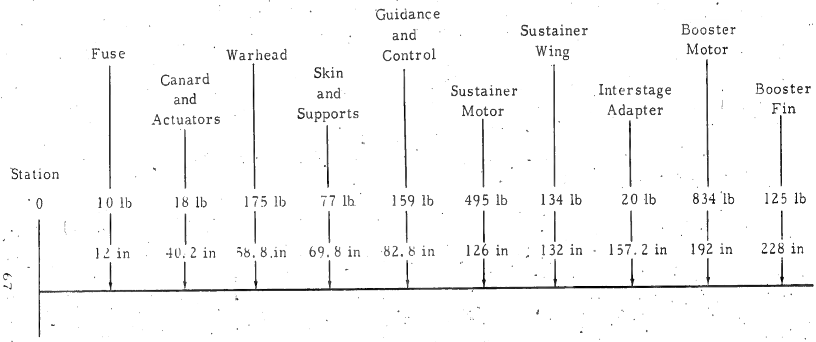

	Station			
Boost CG at ignition	=	147.1 in	or	12.25 ft
Boost CG at burnout	=	131.9 in	or	10.99 ft
Sustainer CG at ignition	=	102.4 in	or	8.53 ft
Sustainer CG at burnout	=	92.2 in	or	7.68 ft

Sustainer weight	1068 lb
Booster Weight	979 lb
Total Missile Weight	2047 lb

Figure 34. (S) Estimated Component Locations and Weights. (U)

control fin deflection angle is required to maintain a given trim angle of attack. The allowable angle of attack increases with altitude but decreases with increasing Mach number since the normal force is proportional to the dynamic pressure.

c. (S) Figure 33 may be misleading unless the particular conditions used for the computations are kept in mind. The Mach number range of 2.2 to 2.7 at sustainer burnout is based on minimum drag from a zero-lift trajectory. Drag will increase sharply with angle of attack. Experimental data based on wind tunnel testing of the sustainer configuration are necessary to determine the drag curve as a function of angle of attack for the low supersonic and transonic regimes. Theoretical approaches are not sufficiently accurate to warrant computations of the effects of maneuvers on missile velocity before or after sustainer burnout. The computations that can be obtained for zero-lift trajectories do provide a reasonable basis for estimating a maximum altitude capability of approximately 35,000 feet and a slant range capability of approximately 12 nm.

APPENDIX III. (S) FLAT FACE RADAR (C)

A. (S) Description (U)

(S) The FLAT FACE is a medium-range, low-altitude, surveillance radar. This radar has two elliptical paraboloid reflectors, each approximately 7 feet by 18 feet, mounted horizontally one above the other atop a box-bodied ZIS-151 Van. This radar is considered to have an effective low-altitude search capability and probably has anticlutter circuits to minimize ground returns and some ECM.

B. (S) Technical Characteristics (U)

RF	815-845, 880-915 Mcs
PRF	480-520, 630-710 pps
PW	1.5-2.5 μsec
Scan	Circular 8.5-9.3 spr
HBW	4.5-11.0°
Polarization	Horizontal

APPENDIV IV. (S) POSTULATED GUIDANCE SYSTEM (U)

(S) A postulated beam-rider guidance system compatible with both the GOA missile electronics and the general configuration of the probable fire control radar, LOW BLOW (characteristics unknown, see MIS 31-63, "Sino-Soviet Block Missile and Space Technology - Summary 1963"), is described below. In general terms, the target track radar would acquire and track the target making it possible to determine the launch time. After launch, the missile would derive its guidance signals from a conically scanned beam transmitted by the missile guidance radar. The target tracking radar could employ two troughs and a dish antenna. Another dish antenna could function with the missile guidance radar. The antennas for both radars could be mounted on a single pedestal.

1. (S) Target Track Radar (U)

a. (S) This radar probably can function as limited acquisition type while transmitting energy at a lower PRF than that used during the guidance mode. It can be expected to operate similar to the FAN SONG in that a guidance officer initially chooses the target of interest from data derived by the LOW BLOW radar or from some other acquisition radar (FLAT FACE) operating in the vicinity. After acquisition, operators probably manually track the target using scopes. An automatic tracking mode would be expected, although this mode would be dependent upon clutter return and jamming signals. In case of jamming, alternate frequencies could be utilized since, in the system being described, the missile is not in any way dependent on the target track radar frequency for its guidance. Circular polarization of the transmitted energy from the LOW BLOW would be expected. This would allow the use of one transmitter for tracking purposes with the troughs receiving the reflected energy. Since estimates of the maximum range of the missile appear to be not greater than approximately 12 nm, a PRF in the range of 5000 to 3750 might be expected which would give an unambiguous range of 16 to 22 nm. A lower PRF of 2500 to 1875 might also be expected for the acquisition mode of operation for ranges of 32 to 43 nm, respectively. If the PRF is changed from acquisition to guidance modes, the receiver bandwidth and pulse width might also be changed as in the FAN SONG.

b. (S) This radar would have advantages at low look angles in a clutter environment because the expected higher PRF would permit the use of narrower range gates. A second advantage would be the probable incorporation of narrower receiver bandwidths

since the reception of a beacon signal for the missile is not a requirement in this guidance scheme. More clutter energy is returned from horizontal rather than vertical polarized energy, therefore, the arrangement of the troughs (45° from horizontal) on the LOW BLOW may be a compromise between the two.

2. (S) Missile Guidance Radar (U)

a. (S) This radar is expected to radiate either one or two beams of conically scanned energy; however, for the purpose of presenting a postulated guidance scheme, a system is described which uses two beams, each operating at different frequencies. The first beam would be radiated at a frequency designated f_1 and would be relatively large in width and of lower power density than the second beam. The second beam, frequency designated f_2, would be narrower in width and its beam center would be offset from the dish boresight by a much smaller angle than the first. The two beams should be conically scanned at the same rate and any modulation appearing on the radiated beams should be synchronized with the conical scan frequency. The frequency of these two beams would probably not differ by more than a few megacycles. The dish which radiates these beams would be boresighted with the target track radar unless a lead collision course mode were included in the LOW BLOW system. If a lead collision mode were included, the missile guidance dish would be capable of movement in order that its fine beam could be positioned in space at a computed intercept point.

b. (S) During flight the missile would utilize the two beams in the following manner:

(1) (U) Follow an approximately straight flight from launch until entering the broad beam of the missile guidance radar.

(2) (S) Derive course guidance signals from the beam and guide itself to the center of the broad beam, placing it in the narrow beam frequency (f_2). The error deriving circuits would automatically switch from the coarse to the fine beam frequency. The missile would then approach the boresight axis of the guidance dish and proceed toward the target. One possible configuration of the electronic package onboard the missile would consist of the four antennas feeding energy to four pairs of microwave cavities. One cavity in each pair would be tuned to the broad beam frequency (f_1) and the other to the narrow beam frequency (f_2). The output from

these cavities would be amplitude detected and fed to error deriving circuits. The error signals fed to the guidance control components would be determined by the amplitude and phase of the energy detected from the cavities.

c. (S) The cavity pairs onboard the missile could be tuned by plungers attached to gears and driven by a synchro. Another synchro on the external surface in conjunction with some type frequency scale would permit the quick changing of the cavity frequencies to correspond with any change in the broad and narrow beam frequencies of the missile guidance radar. Such a device could be located within the box on the interstage section of the missile (Figure 9).

d. (S) As indicated in the analysis of the polyrod antennas, the center frequency is approximately 2.7 gigacycles. If the guidance scheme described herein is used, the frequency of the transmitted energy from the missile guidance radar should be about 2.7 gigacycles and scanned at an approximate rate of between 20 and 100 revolutions per second. The transmitted power would be relatively high if the missile package as described was being used. The transmitted power would probably have constant pulses with an amplitude or frequency modulation. Any modulation present should be synchronized with the conical scan frequency.

e. (S) Terminal homing could be incorporated into the missile. If an antenna were placed in the nose section of the missile and its beam offset from the missile longitudinal axis at some squint angle and conically scanned at the same rate as the narrow and broad beams of the guidance radar; then terminal homing guidance could be accomplished using the same error deriving circuits as used during the initial stage of flight. This antenna could operate at the frequency of the target track radar by including another cavity onboard tuned to this frequency.

f. (S) The guidance scheme described would allow several missiles to be fired at a target or group of targets. Some time should elapse between firings to prevent a missile disturbing the guidance radar radiation pattern for other missiles fired at the same target.

APPENDIX V. (U) REFERENCES (U)

1. Pitts, William C., Nielson, and George E. Kaattari, "Lift and Center of Pressure of Wing-Body-Tail Combinations at Subsonic, Transonic, and Supersonic Speeds", NACA Report No. 1307, 1959

2. Love, Eugene S., "Base Pressure at Supersonic Speeds of Two-Dimensional Airfoils and on Bodies of Revolution With and Without Fins Having Turbulent Boundary Layers", NACA TN 3819, 1957

3. Krost, H. H., W. L. Chow, and G. W. Tumwalt, "Research on Transonic and Supersonic Flow of a Real Fluid at Abrupt Increase in Cross Section", University of Illinois ME TR 392-5

4. Spearman, M. Leroy, "Aerodynamic Characteristics in Pitch of a Series of Cruciform-Wing Missiles with Canard Controls at a Mach Number of 2.01", NASA TN D-839, May, 1961

5. Love, Eugene S., "Experimental and Theoretical Studies of Axisymmetric Free Jets", NASA TR R-6, 1959

6. Chow, W. L. and A. L. Addy, "Interaction Between Primary and Secondary Streams of Supersonic Ejector Systems and Their Performance", AIAA Journal, 2, April, 1964

APPENDIX VI. (U) DISTRIBUTION LIST (U)

	Number of Copies
State Department	1
Central Intelligence Agency	15
National Security Agency	5
National Indications Center	1
U.S. Intelligence Board	3
(GMAIC)	(1)
(JAEIC)	(1)
(SIC)	(1)
National Photographic Interpretation Center	5
Military Liaison to Atomic Energy Commission	1

****

Naval Intelligence	20
U.S. Naval Photographic Interpretation Center	2

****

25X1C

[redacted]	10
	6

****

USAF Foreign Technology Division	5
Air Force Intelligence	20

****

Joint Chiefs of Staff, Technical Intelligence Branch, J-2	2
Defense Intelligence Agency	24
OFFUT Air Force Base, JLED 129	1
CIA/DIA Joint Analysis Group	1

****

Undersecretary of the Army	1
Assistant Secretary, Research and Development	2
Deputy Chief of Staff, Military Operations	3

DISTRIBUTION LIST (Continued)

	Number of Copies
Assistant Chief of Staff, Force Development . . .	3
Chief, Research and Development	3
Office of Assistant Chief of Staff for Intelligence .	10
(ACSI Scientific Advisor)	(1)
(DSR for SpAD)	(1)
(World Wide Division)	(1)
(Scientific and Technical Division)	(1)
(DPP&A)	
(Intelligence Documents Branch)	(2)
(U.S. Army Imagery Interpretation Center)	(3)
U. S. Army Europe	15
U. S. Army Pacific	10
XVIII Airborne Corps	3
U. S. Army Materiel Command	5
U. S. Army Mobility Command.	1
U. S. Army Munitions Command	1
U. S. Army Weapons Command	1
U. S. Army Test and Evaluation Command	2
U. S. Army Electronics Command	2
Headquarters, U. S. Army Air Defense Command	1
CG, Carlisle Barracks, Pa., Attn; Ons Gp. Sec 6	1
CG, Fort Ritchie, Md., Attn: Det F, Sec 9	1
CG, Aberdeen Proving Ground, Maryland	3
U. S. Army Arsenal, Frankfort	1
U. S. Army Combat Development Command . . .	5
U. S. Army Combat Development Command Artillery Agency	1
U. S. Army Combat Development Command Air Defense Agency.	1
U. S. Army Security Agency.	1
Harry Diamond Laboratories.	2
Foreign Science and Technology Center	10
U. S. Army Intelligence Center	2
U. S. Air Defense School	1
U. S. Army Artillery and Missile School	1
U. S. Army Ordnance Guided Missile School. . .	1
U. S. Army Ordnance School	1
U. S. Army Intelligence School.	1
U. S. Army Aviation Center	1
U. S. Army Artillery Board	1

DISTRIBUTION LIST (Continued)

	Number of Copies
U. S. Army Air Defense Board.	1
U. S. Army Airborne and Electronics Board. . .	1
U. S. Army Aviation Board	1
Director, Special Weapons Development.	1
U. S. Army Missile Command	43
(AMCPM-MB)	(1)
(AMCPM-ZER-T)	(1)
(AMCPM-PE)	(1)
(AMCPM-SE)	(1)
(AMCPM-HE)	(1)
(AMCPM-HA)	(1)
(AMCPM-MA)	(1)
(AMSMI-R)	(15)
(AMSMI-I)	(1)
(AMSMI-S)	(1)
(AMSMI-XE)	(1)
(AMSMI-XS)	(1)
(AMSMI-XGM)	(1)
(AMSMI-XBT)	(1)
(AMSMI-XBH)	(1)
(AMSMI-Y)	(12)
(Electronic Defense Laboratories, Sylvania)	(1)
(Electromagnetic Systems Laboratory, Inc.)	(1)
	268

WARNING NOTICE

THIS DOCUMENT CONTAINS INFORMATION AFFECTING THE NATIONAL DEFENSE OF THE UNITED STATES WITHIN THE MEANING OF THE ESPIONAGE LAWS, (18 USC 793,794), THE TRANSMISSION OR REVELATION OF WHICH IN ANY MANNER TO AN UNAUTHORIZED PERSON IS PROHIBITED BY LAW.

SECRET

S-	
int/	date
INDEXED PG	23 MAR 65
CODED DU	23 MAR
CHECKED	2 ... 65
RELEASED	

SECRET

SECRET

S-	
int/	date
INDEXED	
YG	23 MAR 65
CODED	
DLC	23 Mar
CHECKED	
	Mar 65
RELEASED	

SECRET